

pQCD meets phase quenching: the pressure of cold quark matter

August 21, 2024

Kaapo Seppänen

kaapo.seppanen@helsinki.fi

In collaboration with R. Paatelainen and P. Navarrete

[2403.02180]



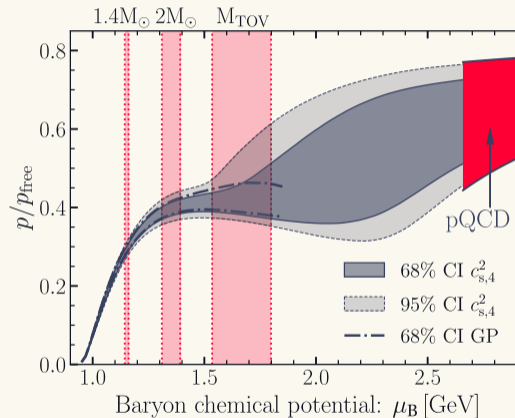
HELSINGIN YLIOPISTO
HELSINGFORS UNIVERSITET
UNIVERSITY OF HELSINKI



Cold and dense pQCD and phase quenching

QCD thermodynamics at high density

- Thermodynamics of cold quark matter ($T = 0, \mu_B \neq 0$) is largely unknown due to the Sign Problem of lattice field theory
- Perturbative QCD viable at high baryon chemical potential μ_B and zero temperature T as QCD coupling $\alpha_s \ll 1$
- **High-order corrections to pQCD pressure constrain the neutron-star equation of state** Komoltsev & Kurkela PRL '22



(adapted from Annala et al. Nat. Com. '23)

Framework for calculating cold and dense pQCD pressure

- 1 Generate Feynman diagrams from partition function:

$$p(\mu) \sim \ln Z = \ln \int \mathcal{D}\bar{\psi}\psi A e^{-S_{\text{QCD}}}$$

$$p_{\text{QCD}} \equiv \text{[Feynman diagrams]} + \dots$$

The diagram shows the pQCD pressure as a sum of Feynman diagrams. The first diagram is a fermion loop (a circle with two arrows pointing in opposite directions). The second diagram is a fermion loop with a wavy gluon line connecting the two vertices. This is followed by an ellipsis indicating higher-order diagrams.

- Fermionic 4-momenta at finite density: $P = (p_0 + i\mu, \vec{p})$

Framework for calculating cold and dense pQCD pressure

- 1 Generate Feynman diagrams from partition function:

$$p(\mu) \sim \ln Z = \ln \int \mathcal{D}\bar{\psi}\psi A e^{-S_{\text{QCD}}}$$

$$p_{\text{QCD}} \equiv \text{[Feynman diagrams]} + \dots$$
The diagram shows the expansion of the pQCD pressure. It starts with an equals sign followed by a fermion loop (a circle with two arrows indicating a clockwise path). This is followed by a plus sign, then a fermion loop with a wavy gluon line connecting two vertices on the loop. This is followed by another plus sign and an ellipsis.

- Fermionic 4-momenta at finite density: $P = (p_0 + i\mu, \vec{p})$

- 2 Calculate multi-loop integrals in dimensional regularization

Framework for calculating cold and dense pQCD pressure

- 1 Generate Feynman diagrams from partition function:

$$p(\mu) \sim \ln Z = \ln \int \mathcal{D}\bar{\psi}\psi A e^{-S_{\text{QCD}}}$$

$$p^{\text{pQCD}} \equiv \text{[fermion loop]} + \text{[gluon loop]} + \dots$$

- Fermionic 4-momenta at finite density: $P = (p_0 + i\mu, \vec{p})$

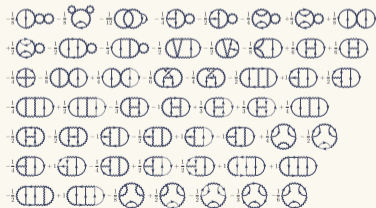
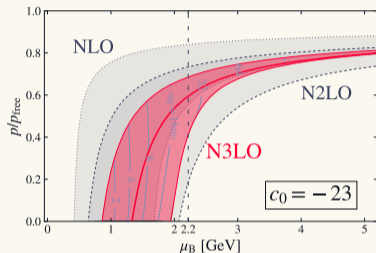
- 2 Calculate multi-loop integrals in dimensional regularization

Resummations required due to IR divergences associated with in-medium screening
 $\Rightarrow \ln \alpha_s$ in perturbative expansion (Saga's talk)

Partial N³LO pressure of cold and dense QCD

$$\frac{p}{p_{\text{free}}} = 1 + c_1 \alpha_s + (c_{2,1} \ln \alpha_s + c_{2,0}) \alpha_s^2 + (c_{3,2} \ln^2 \alpha_s + c_{3,1} \ln \alpha_s + c_{3,0}) \alpha_s^3 + O(\alpha_s^4)$$

- $c_1, c_{2,1}, c_{2,0}$: B. Freedman & L. McLerran PRD '77
- $c_{3,2}$: S. Säppi et al. PRL '18, S. Säppi et al. PRL '21
- $c_{3,1}$: T. Gorda, R. Paatelainen, S. Säppi, K.S., PRL '23
- $c_{3,0}$: 52 4-loops, work in progress...



Phase quenching

- Provides an alternative nonperturbative way of determining the cold and dense pQCD pressure Moore & Gorda JHEP '23, Fujimoto & Reddy PRD '24
- QCD partition function:

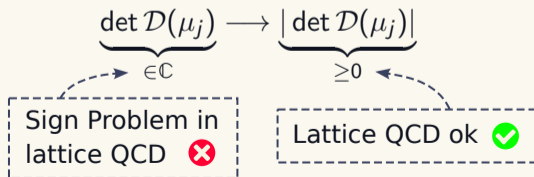
$$Z_{\text{QCD}}(\vec{\mu}) = \int \mathcal{D}A e^{-S[A]} \prod_{j=1}^{N_f} \det \underbrace{\mathcal{D}(\mu_j)}_{\not{D} + m + \mu_j \gamma^0}$$

Phase quenching

- Provides an alternative nonperturbative way of determining the cold and dense pQCD pressure Moore & Gorda JHEP '23, Fujimoto & Reddy PRD '24
- QCD partition function:

$$Z_{\text{QCD}}(\vec{\mu}) = \int \mathcal{D}A e^{-S[A]} \prod_{j=1}^{N_f} \det \underbrace{\mathcal{D}(\mu_j)}_{\not{D} + m + \mu_j \gamma^0}$$

- Phase quenching:



Upper bound for full QCD

- Upper bound for Z_{QCD} and pressure $p_{\text{QCD}} \sim \ln Z_{\text{QCD}}$

$$Z_{\text{QCD}}(\vec{\mu}) \leq Z_{\text{PQ}}(\vec{\mu}) \quad \Rightarrow \quad p_{\text{QCD}}(\vec{\mu}) \leq p_{\text{PQ}}(\vec{\mu})$$

- Turning the inequality into an equality

$$\underbrace{p_{\text{PQ}}(\vec{\mu})}_{\text{lattice QCD}} - \underbrace{p_{\text{QCD}}(\vec{\mu})}_{?} = \underbrace{\text{positive number}}_{\text{easier to compute than } p_{\text{QCD}}}$$

- The difference between full QCD and phase-quenched QCD can be computed perturbatively at high densities where $\alpha_s \ll 1$

\Rightarrow Solve for p_{QCD} !

Phase-quenched Feynman rules

- γ^5 -hermiticity of the Dirac operator:

$$\gamma^5 \mathcal{D}(\mu_j) \gamma^5 = \mathcal{D}^\dagger(-\mu_j) \quad \Rightarrow \quad [\det \mathcal{D}(\mu_j)]^* = \det \mathcal{D}(-\mu_j)$$

- Phase-quenched determinant:

$$|\det \mathcal{D}(\mu_j)| = \sqrt{\det \mathcal{D}(-\mu_j) \det \mathcal{D}(\mu_j)} = \exp \left\{ \frac{1}{2} \left[\text{tr} \ln \mathcal{D}(-\mu_j) + \text{tr} \ln \mathcal{D}(\mu_j) \right] \right\}$$

\Rightarrow average over $\pm\mu_j$ in quark loops

Phase-quenched Feynman rules

- γ^5 -hermiticity of the Dirac operator:

$$\gamma^5 \mathcal{D}(\mu_j) \gamma^5 = \mathcal{D}^\dagger(-\mu_j) \quad \Rightarrow \quad [\det \mathcal{D}(\mu_j)]^* = \det \mathcal{D}(-\mu_j)$$

- Phase-quenched determinant:

$$|\det \mathcal{D}(\mu_j)| = \sqrt{\det \mathcal{D}(-\mu_j) \det \mathcal{D}(\mu_j)} = \exp \left\{ \frac{1}{2} \left[\text{tr} \ln \mathcal{D}(-\mu_j) + \text{tr} \ln \mathcal{D}(\mu_j) \right] \right\}$$

\Rightarrow average over $\pm\mu_j$ in quark loops

- PQ Feynman rule (recall $P = (p^0 + i\mu_j, \vec{p})$ for fermions):

$$\left[\text{quark loop} \right]_{\text{PQ}} = \frac{1}{2} \left\{ \left. \text{quark loop} \right|_{i\mu_j \rightarrow -i\mu_j} + \text{quark loop} \right\} = \text{Re} \left[\text{quark loop} \right]$$

$p_{\text{PQ}} - p_{\text{QCD}}$ perturbatively

- Vacuum-type diagrams are real due to symmetry under $i\vec{\mu} \rightarrow -i\vec{\mu}$
- Single-quark-loop diagrams are the same in phase-quenched and full QCD, e.g.

$$\left[\text{Diagram} \right]_{\text{PQ}} - \left[\text{Diagram} \right]_{\text{QCD}} = \text{Re} \left[\text{Diagram} \right] - \left(\text{Re} \left[\text{Diagram} \right] + \underbrace{i \text{Im} \left[\text{Diagram} \right]}_{=0} \right) = 0$$

\Rightarrow The difference has to contain at least **two quark loops**

- First two-quark-loop diagram appears at three loops:

$$\begin{aligned}
 & \left[\text{Diagram} \right]_{\text{PQ}} - \left[\text{Diagram} \right]_{\text{QCD}} \\
 &= \left(\text{Re} \text{ Re} \right) - \left(\text{Re} \text{ Re} + 2i \underbrace{\text{Re} \text{ Im}}_{=0} - \text{Im} \text{ Im} \right) \\
 &= \text{Im} \text{ Im}
 \end{aligned}$$

The diagrams are two-loop diagrams with a central wavy line and two circular loops on either side. In the first row, the loops are empty. In the second row, the left loop is labeled 'Re' and the right loop is labeled 'Re'. In the third row, the left loop is labeled 'Re' and the right loop is labeled 'Im'. In the final row, both loops are labeled 'Im'.

- But the one-loop two-gluon function is real ($P^0 = p^0 + i\mu$):

$$\Gamma_{\alpha\beta}^{(2)}(\mu, Q) \equiv \int_{\{P\}} \frac{\text{tr}[\not{P}\gamma_\alpha(\not{P} - \not{Q})\gamma_\beta]}{P^2(P - Q)^2} \stackrel{P \rightarrow Q-P}{=} \Gamma_{\alpha\beta}^{(2)}(\mu, Q)^* \Rightarrow \text{Im} = 0$$

$$\Rightarrow \text{Im} = 0$$


- But the one-loop two-gluon function is real ($P^0 = p^0 + i\mu$):

$$\Gamma_{\alpha\beta}^{(2)}(\mu, Q) \equiv \int_{\{P\}} \frac{\text{tr}[\not{P}\gamma_\alpha(\not{P} - \not{Q})\gamma_\beta]}{P^2(P - Q)^2} \stackrel{P \rightarrow Q-P}{=} \Gamma_{\alpha\beta}^{(2)}(\mu, Q)^* \Rightarrow \text{Im} = 0$$

$$\Rightarrow \text{Im} = 0$$


- No such symmetries for one-loop three-gluon function $\Rightarrow \text{Im} \neq 0$

$$\Rightarrow \text{Im} \neq 0$$

\Rightarrow The difference has to contain at least **two three-gluon functions**

$p_{\text{PQ}} - p_{\text{QCD}}$ perturbatively at $O(\alpha_s^3)$

- First nonzero contribution to $p_{\text{PQ}} - p_{\text{QCD}}$ at four-loop order, “Bugblatter” Moore & Gorda JHEP '23:

$$\underbrace{p_{\text{PQ}}(\mu_B)}_{\text{lattice QCD}} - \underbrace{p_{\text{QCD}}(\mu_B)}_{?} = \text{Diagram} + O(\alpha_s^4)$$


$$\propto \alpha_s^3 d^{abc} d^{abc} N_f^2 \int_{QS} \frac{[\text{Im} \Gamma_{\mu\nu\sigma}^{(3)}(\mu_B, Q, S)]^2}{Q^2 S^2 (Q - S)^2} + O(\alpha_s^4)$$

- Beta-equilibrium at high densities $\Rightarrow \mu_j = \mu_B / N_c$ for $j \in \{u, d, s\}$
- UV and IR finite, positive, and gauge-invariant number

\Rightarrow Full $O(\alpha_s^3)$ pressure from single four-loop diagram + PQ lattice result

Multiloop integration techniques at finite density

Traditional multiloop techniques at $\mu = 0$

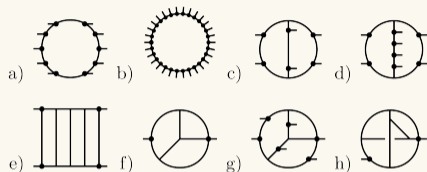
- Significant advancements in multiloop integration techniques for collider physics at $\mu = 0$ over the last decades
- Many traditional state-of-the-art methods rely on Lorentz symmetry:
 - Integration by parts for a reduction to master integrals
 - Differential equations
 - Sector decomposition
 - etc.
- Major obstacle at finite μ : **broken Lorentz symmetry** due to $p^0 \rightarrow p^0 + i\mu$ for fermions

Seems like we are stuck...

Are there any powerful $\mu = 0$ methods that generalize to $\mu > 0$?

Inspiration from Loop-Tree Duality at $\mu = 0$

- Direct numerical integration in momentum space using the Loop-Tree Duality:
 - 1 All energy integrals computed analytically with residue theorem
 - 2 Remaining spatial momentum integrals computed numerically using Monte Carlo integration
- 0-components singled out \Rightarrow naturally generalizes to finite μ where $p^0 \rightarrow p^0 + i\mu$



| G | Reference | Numerical LTD | N [10^6] | $[\mu\text{s}]$ |
|-----|---------------------------------|-------------------------------|----------------|-----------------|
| a)* | [33] $i4.31638 \cdot 10^{-7}$ | $i4.31637(19) \cdot 10^{-7}$ | 110 | 1.1 |
| b) | [33] $i0.358640$ | $i0.358646(29)$ | 210 | 5.9 |
| c) | [7] $1.1339(5) \cdot 10^{-4}$ | $1.133719(58) \cdot 10^{-4}$ | 5500 | 2.5 |
| c)* | [7] $4.398(1) \cdot 10^{-8}$ | $4.39825(17) \cdot 10^{-8}$ | 5500 | 2.5 |
| d)* | [7] $2.409(1) \cdot 10^{-8}$ | $2.40869(27) \cdot 10^{-8}$ | 5500 | 3.5 |
| e) | [34] $-1.433521 \cdot 10^{-6}$ | $-1.4338(18) \cdot 10^{-6}$ | 1500 | 27.4 |
| f) | [35] $i5.26647 \cdot 10^{-6}$ | $i5.236(38) \cdot 10^{-6}$ | 7000 | 3.3 |
| g)* | [7] $i1.7790(6) \cdot 10^{-10}$ | $i1.77648(48) \cdot 10^{-10}$ | 22000 | 11 |
| h) | [35] $-8.36515 \cdot 10^{-8}$ | $-8.309(31) \cdot 10^{-8}$ | 7000 | 15.8 |

Z. Capatti et al. PRL '19

Representations for the spatial integrands

- 3d integrands obtained after energy integrations can be written using different representations:
 - Loop-Tree Duality (LTD), Cross-Free Family (CFF), Time-Ordered Pert. Theory,...
 - Choice of the representation affects the performance of numerical integration
- We generalize the CFF representation by [Z. Capatti PRD '23](#) to finite μ
 - We call it the **dense Loop-Tree Duality (dLTD)** [K.S.](#), [R. Paatelainen](#), [P. Navarrete \[2403.02180\]](#)
 - No spurious singularities unlike in the finite-density cutting rules

l -loop vacuum-type integral at finite chemical potential μ with n propagators:

$$I \equiv \int \left[\prod_{i=1}^l \frac{d\mathbf{p}_i^0}{2\pi} \right] \frac{\mathcal{N}(\mathbf{Q}^0)}{\prod_{j=1}^n [(Q_j^0)^2 + E_j^2]}$$

- Bold symbols = n -dimensional vectors
- $\mathbf{Q}^0 = \sum_{i=1}^l \mathbf{S}_i p_i^0 + i\boldsymbol{\tau}\mu$ = frequencies of the propagators
- $\mathbf{S}_i \in \{\pm 1, 0\}^n$ = vectors that fix the loop momentum basis
- $\boldsymbol{\tau} = \sum_{i=1}^l \mathbf{S}_i \tilde{\tau}_i \in \{\pm 1, 0\}^n$ with $\tilde{\tau}_i \in \mathbb{Z}$ = fermion signature vector
- \mathcal{N} = multilinear polynomial

dLTD derivation: Performing the 0-component integrals

Insert the following unity for each propagator j in I :

$$1 = \int d\tilde{p}_j^0 \delta \left(\tilde{p}_j^0 - \sum_{i=1}^l S_{ji} p_i^0 \right)$$

and write the delta functions as integrals over α_j (Fourier representation)

$$I = \int \prod_{i=1}^l \frac{dp_i^0}{2\pi} \int \prod_{j=1}^n d\alpha_j e^{-i\alpha_j \sum_{i=1}^l S_{ji} p_i^0} \int \left[\prod_{j=1}^n \frac{d\tilde{p}_j^0}{2\pi} \frac{e^{i\alpha_j \tilde{p}_j^0}}{(\tilde{p}_j^0 + i\tau_j \mu)^2 + E_j^2} \right] \mathcal{N}(\tilde{\mathbf{p}}^0 + i\tau \mu)$$

\Rightarrow 0-component integrals over \tilde{p}_j^0 can be performed independently for each propagator

dLTD derivation: Final result

Using the residue theorem, we obtain the final result


$$I = \sum_{\rho, \sigma \in \{\pm 1\}^n} \mathcal{N}(i\sigma \odot \rho \odot \mathbf{E}) \prod_{j=1}^n \frac{\Theta(\rho_j E_j - \sigma_j \tau_j \mu)}{2\rho_j E_j} \underbrace{\int_{\mathbb{R}_+^n} d\alpha e^{-\alpha \cdot (\rho \odot \mathbf{E})} \prod_{i=1}^l \delta(\alpha \cdot (\sigma \odot \mathbf{S}_i))}_{= \text{some rational function of } E_j \text{'s, no } \mu \text{-dependence!}}$$

- Difference to the $\mu = 0$ case:
 - Step functions with a chemical potential μ
 - Additional sum over sign vectors ρ
- α -integral is a Laplace transform of a nonsimplicial convex cone
 - The same integral already appears in the $\mu = 0$ case
 - Closed-form solution using diagrammatic algorithm by [Z. Capatti PRD '23](#)

Example: two-loop sunset

$$\int \left[\prod_{i=1}^l \frac{d\rho_i^0}{2\pi} \right] \frac{\mathcal{N}(\mathbf{Q}^0)}{\prod_{j=1}^n [(Q_j^0)^2 + E_j^2]} = \sum_{\rho, \sigma \in \{\pm 1\}^n} \mathcal{N}(i\sigma \odot \rho \odot \mathbf{E}) \prod_{j=1}^n \frac{\Theta(\rho_j E_j - \sigma_j \tau_j \mu)}{2\rho_j E_j} \int_{\mathbb{R}_+^n} d\alpha e^{-\alpha \cdot (\rho \odot \mathbf{E})} \prod_{i=1}^l \delta(\alpha \cdot (\sigma \odot \mathbf{S}_i))$$

- $l = 2$, $n = 3$, $\mathbf{S}_1 = (1, 0, 1)$, $\mathbf{S}_2 = (0, 1, -1)$, $\boldsymbol{\tau} = (1, 1, 0)$,
 $\mathbf{E} = (|\vec{p}_1|, |\vec{p}_2|, |\vec{p}_1 - \vec{p}_2|)$
- Performing the α -integrals for the sunset yields four distinct nonvanishing terms



$$\propto \int \frac{d^3 \vec{p}_1}{(2\pi)^3} \frac{d^3 \vec{p}_2}{(2\pi)^3} \left\{ \frac{(E_1 E_2 + \vec{p}_1 \cdot \vec{p}_2) \Theta(E_1 - \mu)}{2E_1 2E_2 2E_3 (E_1 + E_2 + E_3)} - \frac{(-E_1 E_2 + \vec{p}_1 \cdot \vec{p}_2) \Theta(E_1 - \mu) \Theta(-E_2 + \mu)}{2E_1 2E_2 2E_3 (E_1 - E_2 + E_3)} + (1 \leftrightarrow 2) \right\}$$




- For numerical integration, UV divergences are subtracted with local counterterms using BPHZ R-operation

Numerical integration & benchmarks

- Spatial loop momenta \vec{p}_i parametrized using spherical coordinates
- Numerical integration of spatial momentum integrals using Vegas
- Multichannel approach implemented for flattening integrable singularities (see Z. Capatti et al. JHEP '20)

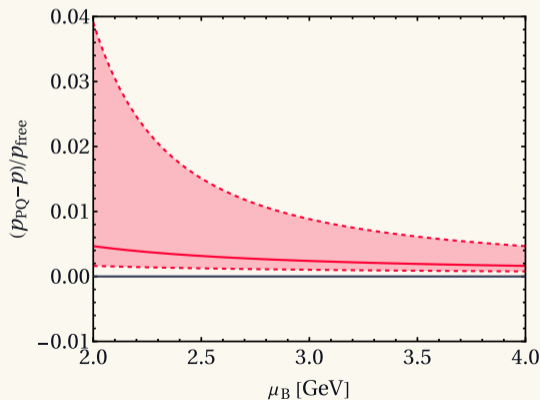
Numerical integration & benchmarks

- Spatial loop momenta \vec{p}_i parametrized using spherical coordinates
- Numerical integration of spatial momentum integrals using Vegas
- Multichannel approach implemented for flattening integrable singularities (see Z. Capatti et al. JHEP '20)

| | Diagram | Analytic | dLTD | $N [10^6]$ | $[\mu\text{s}]$ |
|---------------------------------|---|-------------------------|----------------------------|------------|-----------------|
| Massive scalars at $\mu = 0$ |  | $2.16928 \cdot 10^{-9}$ | $2.16931(4) \cdot 10^{-9}$ | 3000 | 5.2 |
| |  | -0.00128325 | $-0.00128338(23)$ | 150 | 5.8 |
| QCD at $\mu > 0$ |  | -0.000256547 | $-0.00025654(9)$ | 800 | 9.6 |

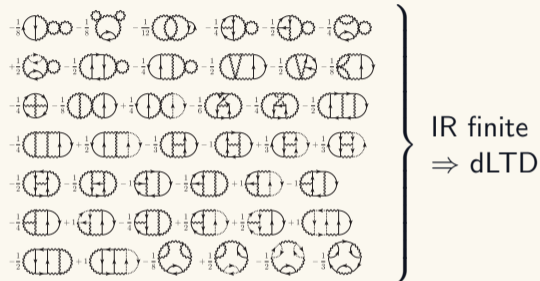
Result for $p_{\text{PQ}} - p_{\text{QCD}}$ using dLTD

$$p_{\text{PQ}}(\mu_{\text{B}}) - p_{\text{QCD}}(\mu_{\text{B}}) = 3.368(7) \cdot \left(\frac{\alpha_{\text{S}}}{\pi}\right)^3 p_{\text{free}} + O(\alpha_{\text{S}}^4)$$



- dLTD representation of the Bugblatter integrated using $6 \cdot 10^{11}$ MC samples
- First ever computation of 2PI four-loop diagram at finite μ_{B}
- Small number compared to the known perturbative coefficients at $O(\alpha_{\text{S}}^3)$
- **Conclusion:** Phase-quenched lattice can provide a complementary method for determining the pressure of cold quark matter at high μ_{B}

Next: Applying dLTD to computing $c_{3,0}$ directly



Summary

- pQCD constrains the neutron-star equation of state
- $O(\alpha_s^3)$ cold and dense QCD pressure can be determined from phase-quenched lattice simulations + our new four-loop result
- Powerful numerical tool from collider physics generalized to finite μ : direct numerical integration of Feynman diagrams in momentum space using the dense Loop-Tree Duality

- pQCD constrains the neutron-star equation of state
- $O(\alpha_s^3)$ cold and dense QCD pressure can be determined from phase-quenched lattice simulations + our new four-loop result
- Powerful numerical tool from collider physics generalized to finite μ : direct numerical integration of Feynman diagrams in momentum space using the dense Loop-Tree Duality

Thanks for your attention!

Extra slides

Future directions for dLTD

Finite temperature

- Already benchmarked at 2-loops
- $\Theta \rightarrow n_{B/F}$

UV/IR subtractions

- All-orders automatization of UV-subtraction nearly complete
- IR HTL-counterterms at $T = 0, \mu > 0$



Performance

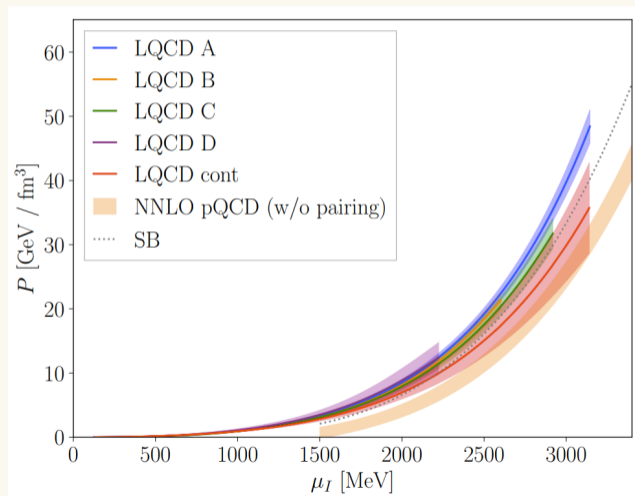
- More efficient sampling methods
- Optimizations

External legs

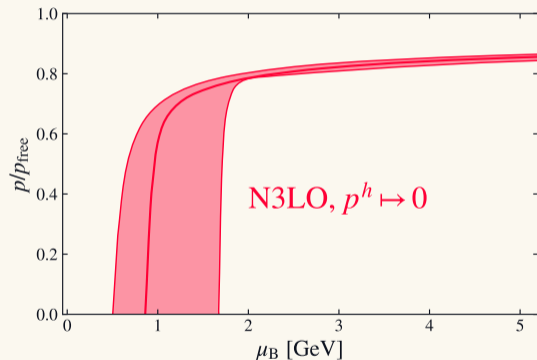
- Real-time n -point correlators
- Production rates, etc.

Lattice results for 2 + 1 flavors at finite μ_I

R. Abbott, W. Detmold et al. [2406.09273]:

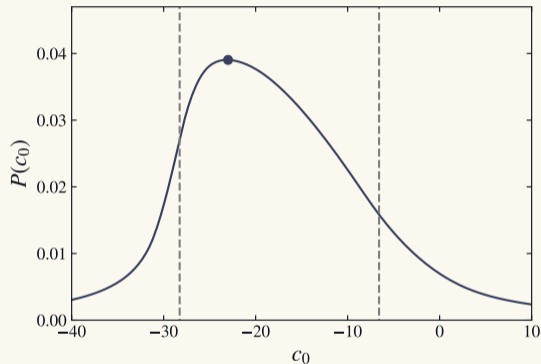


Results for N³LO pressure with only soft and mixed sectors

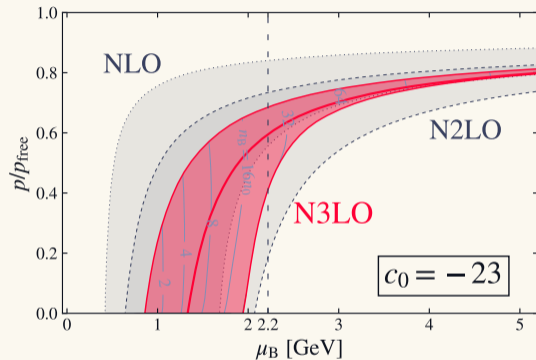


- N³LO result including only screened gluonic sectors (soft+mixed) incredibly well-behaved with nearly vanishing renormalization-scale dependence
- Conclusion: hard sector main source for uncertainty
- Stark contrast to the high- T case

Full N³LO pressure with fixed c_0



- Full N³LO with $c_0 = -23$ most consistent with lower-order results according to Bayesian analysis



- Actual computation of c_0 may lead to a significantly improved EOS usable even at $\mu_B = 2.2$ GeV ($n = 27n_0$), cf. N²LO at $\mu_B = 2.7$ GeV ($n = 40n_0$)